geoconvention
Calgary • Canada • May 15-19 2017

Offset dependent anisotropy analysis in vertically fractured reservoirs: A synthetic study

Sitamai, W. Ajiduah, Gary, F. Margrave and Pat, F. Daley*
CREWES/University of Calgary.

Summary

In this study, we explored and compared seismic amplitude and traveltime behaviours of a 3D-3C HTI anisotropy dataset generated by SINTEF TIGER finite difference modeling and compared the result with Ruger modeling. The anisotropic parameters of the equivalent model were obtained from Schoenberg and Muir linear slip theory and its seismic responses were compared with heterogeneous isotropic model. In this paper, we focused on the reflection amplitude and interval traveltime comparison between these two models and compare the AVO/ AVAZ behavior with Ruger analytical results. We observed that the elastic modeling results and the equivalent results reveals AVAZ signatures which shows more significant azimuthal variations in the elastic model than in the equivalent model. Also, we investigated the effect of mid, near, anf far offset on PP and PS azimuthal anisotropy from the two HTI models with the aim of using the modeling results as guidance in seismic data application. AVO/AVAZ studies show that fracture-induced anisotropy is stronger with increasing offset. We observed that the major axes of the radial-component PS-wave amplitude polarplot point perpendicular to the fracture strike, which is opposite to the PP-wave amplitude polarplot whose major axes are parallel to the fracture strike. We also observed that PP AVAZ behaviour is weaker in the equivalent modeling than in the elastic modeling, however the PS- AVAZ behaviour of both the elastic and equivalent modeling are similar. The interval traveltime azimuthal anisotropy is weak in both models. We infer that P-wave fracture induced anisotropy is weaker in homogeneous equivalent models than in heterogeneous elastic models. Also, PS amplitude anisotropy show an earlier onset of anisotropy and wider offset range than PP anisotropy.

Introduction

Multicomponent seismic exploration has become increasingly important for detecting and characterizing fractured reservoirs. There are various advantages to 3C data, but one of the most important is the use of P and S waves for reservoir characterization – in particular for lithology identification and fracture analysis (Qian et al., 2007; Bale et. al. 2009; Mahmoudian, et. al. 2013; Al Dulaijan et. al. 2016). Fracture analysis is often tackled with P-wave data alone, using velocity or amplitude variation. These require a good distribution of offsets for each azimuth. However, when multi-component data are available, they offer a robust, direct approach to seismic fracture characterization through shear-wave splitting analysis. Shear wave splitting is often indicative of fracturing which can be associated with increased permeability and is a robust tool for characterizing both anisotropy orientation (from the fast (S1) direction) and intensity (from S1-S2 time delay). These are important in understanding fluid pathways in fractured reservoirs. In this paper, we will compare and contrast AVO/AVAZ results and polarplots obtained from (a). Elastic modeling of vertically fractured heterogeneous isotropic model; (b). Equivalent modeling of HTI anisotropic parameters obtained from Schoenberg and Muir (1989) theory for averaging multiple thin isotropic layers, and (c). Ruger modeling of the computed HTI anisotropic parameters obtained from the Schoenberg and Muir equivalent anisotropy computation of (b).

Method.

SINTEF TIGER staggered-grid finite-difference modeling was used to generate 3C-3D synthetic datasets. The datasets were then rotated into radial and transverse component for further analysis. The

model is a 3-layered model; the top layer and bottom layer are isotropic, while the middle layer is a 400m thick HTI layer modeling vertical fracturing. Fracture spacing is at a 20m interval and fracture strike is 0 degrees in the azimuthal plane. The offset range is from 20m to 2000m. The source, an explosive P-source with a 15 Hz Ricker spectrum, is located at the centre of the model, at depth 40m. This gives full azimuthal coverage through all 360 degrees. 3C receivers were placed on each of the grid points and buried at source depth. 3D shot records were generated for both the elastic and the equivalent model. Also, azimuthal variation of PP and PS-converted reflections studies (AVO/AVAZ) and interval traveltime (TVAZ) were analyzed for reflections from the top and bottom of the fractured middle layer. The interval traveltime means the time interval between the top and bottom of the fractured medium. Figure 1a shows a schematic of the equivalent medium theory, figure 1b shows a brief workflow. The parameters of equivalent model and elastic model are shown in Table 1 below.

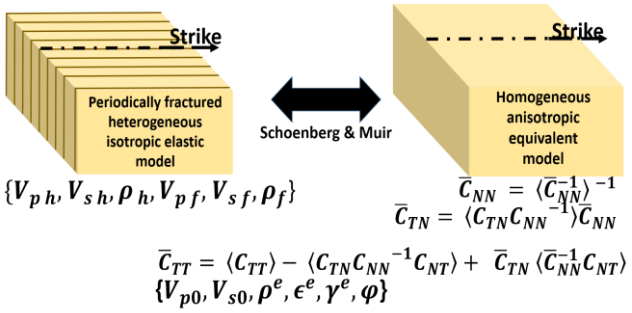

Fig 1a. Schoenberg and Muir Theory

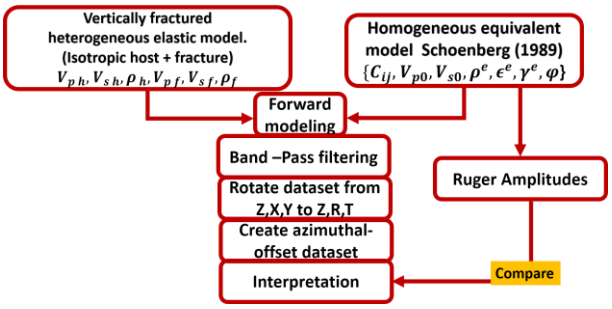

Fig 1b. Workflow

Table 1: Parameters of Model used in modeling.

	Heterogeneous elastic model	Homogeneous equivalent model
Layer1	$Vp = 3500m/s, Vs = 2140m/s, \ \rho = 2200kg/m^3$	same
HTI Layer	$Vp_1 = 4700m/s, Vs_1 = 3980m/s, \rho_1 = 2500kg/m^3$ $Vp_2 = 4210m/s, \ Vs_2 = 2430m/s, \rho_2 = 2300kg/m^3$	$Vp_0 = 4438m/s, Vs_0 = 2762m/s, \rho^e = 2401kg/m^3$ $\epsilon^e = .0034, \gamma^e = .0607, \delta^e = -.0545$
Layer3	$Vp = 5000m/s, Vs = 3300m/s, \rho = 2900kg/m^3$	same

Examples

Figure 2 shows the 2D PP and PS- waves amplitude scans of the vertical (Z), radial (R) and transverse (T) components recorded from the top of the HTI reflector.

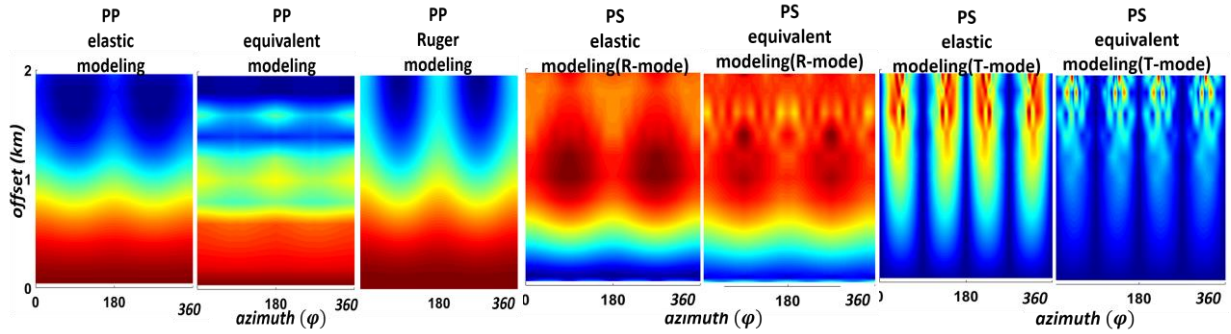

Fig 2. 2D amplitude-offset panels obtained from elastic modeling and equivalent modeling.

The PP- Ruger amplitude modeling (panel 3 of figure 2) obtained from the equivalent model parameters shows strong coherent AVO/AVAZ behaviour and is a close comparison to the finite-difference elastic modeling result (panel 1) which we obtained from using a vertically fractured isotropic heterogeneous elastic model. The finite-difference PP equivalent modeling result (panel 2 of figure 2) show weak fracture-induced anisotropy. A close study of the PS elastic and equivalent modeling (see panel 3,4,5 and 6 of figure 2) show that PS- wave AVAZ responses at offset/depth ratio less than 1 is comparably similar for both elastic and equivalent model. The PS- AVAZ behavior at far offset however, have the same AVAZ pattern with slight difference; the PS- elastic modeling result shows that shear wave splitting of the T mode elastic modeling are clearly distinct at principal orientations than in the equivalent modeling. From this figure, we can infer that P-wave fracture-induced seismic anisotropy is stronger in heterogeneous elastic fractured models than in anisotropic homogenous equivalent models. We also observed that both elastic and equivalent modeling of the converted wave responses show stronger and earlier onset of anisotropy that spans a wider offset than their PP counterparts.

PP and PS azimuthal amplitude anisotropy

Given three different offsets at 0.4, 1, and 1.6km indicated by the blue, red and yellow circles, we picked the azimuthal amplitudes of P and S waves from top of the fractured medium and also computed interval traveltimes within the fractured medium. Figure 3 and 4 shows the azimuthal polarplots at 3 different offsets. The presence of fractures with HTI symmetry cause the amplitude variation with azimuth to deviate from circles to an elliptical form. The longer axis of the PP polarplots (figure 3) point in the direction of strike while in the PS- waves R-mode polarplot, the longer axis point normal to the strike direction (figure 4, panel1). We also see that the Ruger P amplitude modeling and the PP elastic modeling have stronger anisotropy than the equivalent modeling.

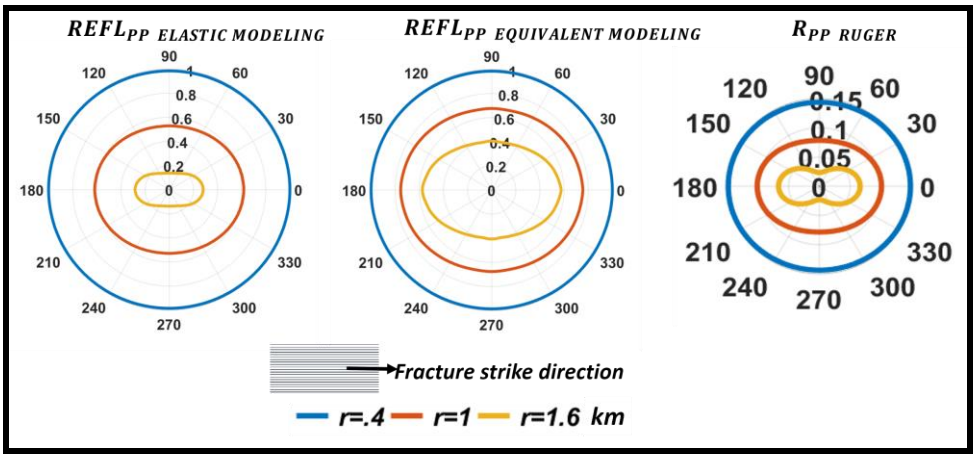

Fig 3. Azimuthal polarplot of PP scaled reflection amplitude azimuthal anisotropy from top of HTI layer for elastic (left) and equivalent modeling (middle) and Ruger (right), major axis is in the fracture strike direction

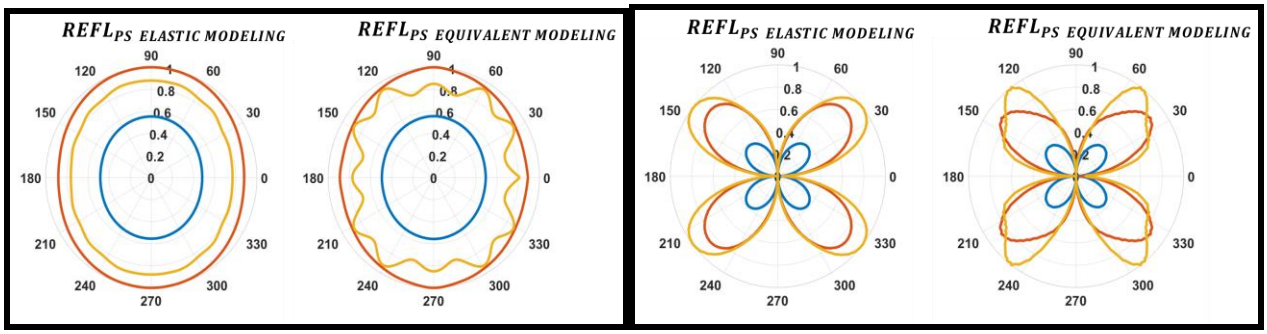

Fig 4. Azimuthal polarplot of PS anisotropy- R-mode (left panel) and T-mode (right panel)

PP and PS azimuthal interval traveltime anisotropy

The two panels of figure 5 are the interval traveltime polarplots of P and PS wave arrivals between the top and bottom of the HTI layer. The PP interval-traveltime plot from equivalent modeling gave no precise fracture direction. We observed that the fracture-induced P-wave traveltime anisotropy in both elastic and equivalent models are not very evident at small offset but may become evident at very large offset as indicated by the yellow ellipse of the elastic modeling. The modeling results shows that the azimuthal variation of interval traveltime of the R-component waves show weak elliptical distribution as well, in both elastic and equivalent models. We infer that the PP and PS amplitudes polarplots are more diagnostic of fracture orientation than their interval traveltime counterparts.

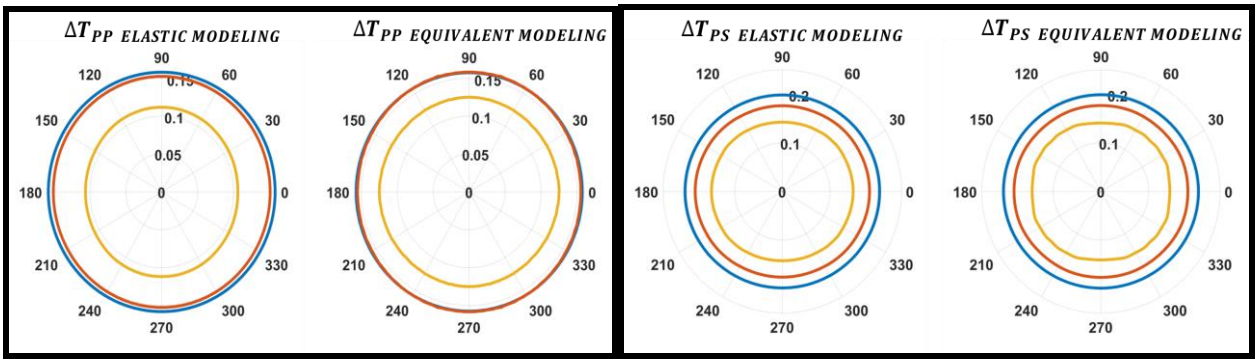

Fig 5. PP (left panel) and PS- wave azimuthal polar plot (right panel) of interval traveltime within the top and bottom of the fractured layer for both elastic and equivalent modeling.

Conclusions

We have studied the offset dependency of AVAZ and TVAZ attributes and explored the advantages of incorporating PS wave analysis into anisotropic studies. We found that PS wave AVAZ analysis show earlier onset of anisotropy than PP- waves. Overall, PP and PS waves AVAZ analysis are better diagnostic tool for fracture orientation detection than traveltime TVAZ analysis. From the offset-azimuth polarplot, we observe that the presence of anisotropy forces an elliptical AVAZ behaviour which are stronger at far offset. AVAZ studies also show the longer axis of PP amplitude polarplot points in the direction of strike and the PS polar plots point normal to the direction of strike. We can conclude that PS anisotropy generally have wider offset range than PP anisotropy. We also observed that the PS azimuthal anisotropy at near, mid and far offsets are similar for both heterogeneous model and homogenous equivalent model, however, the PP azimuthal anisotropy appear vary strongly with azimuths for the heterogeneous elastic model and weak in the homogeneous equivalent model.

Acknowledgements

This work was funded by CREWES industrial sponsors and NSERC (Natural Science and Engineering Research Council of Canada) through the grant CRDPJ 461179-13. The authors also thank SINTEF for providing the TIGER finite-difference modeling software. The first author gratefully acknowledge Kevin Hall, Faranak Mahmoudian and Raul Cova for their assistance.

References

Al Dulaijan and Margrave, G. F. 2016, VVAZ analysis for seismic anisotropy in the Altamont-Bluebell Field, 86th Annual International Meeting, SEG, Expanded Abstracts.

Bale, R., B. Gratakos, B. Mattocks, S. Roche, K. Poplavskii, and X. Li, 2009, Shear wave splitting applications for fracture analysis and improved imaging: Some onshore examples: First Break, 27, 73–83.

Mahmoudian, F., Margrave, G.F., Wong, J., and Henley, D.C, 2013, Fracture orientation and intensity from AVAz inversion: A physical modeling study. 83th Annual International Meeting, SEG, Expanded Abstracts.

Qian, Z., Li, X-Y., Chapman, M., 2007, Azimuthal variations of PP- and PS-wave attributes: a synthetic study: 77th Annual International Meeting, SEG, Expanded Abstracts, 184–187.

Schoenberg, M., and Muir, F., 1989, A calculus for finely layered media: Geophysics, 54, 581–589,